



Do Grain Boundaries Affect Microwave Dielectric Loss in Oxides?

Journal:	<i>Journal of the American Ceramic Society</i>
Manuscript ID:	JACERS-25261.R1
Manuscript Type:	Article
Date Submitted by the Author:	04-Dec-2008
Complete List of Authors:	Breeze, Jonathan; Imperial College London, Materials Perkins, James; Imperial College London, Materials McComb, David; Imperial College London, Materials Alford, Neil; Imperial College London, Department of Materials
Keywords:	dielectric materials/properties, grain boundaries



Preview

Do Grain Boundaries Affect Microwave Dielectric Loss in Oxides?

Jonathan D. Breeze, James M. Perkins, David W. McComb, Neil McN. Alford.

Department of Materials, Imperial College London, London, UK, SW7 2AZ.

Reducing loss in microwave dielectrics is critical to improving performance in wireless communications systems. Grain boundaries in polycrystalline microwave dielectric ceramics have long been suspected of increasing dielectric loss. They are often cited as the main contributor to the observed difference in dielectric losses between single crystals and polycrystalline ceramics. The exact configuration of grain boundaries is problematic to quantify in practice and their influence on the dielectric loss difficult to distinguish from other defects such as porosity, oxygen vacancies, impurities and dislocations. Here we measure the sensitivity of a single grain boundary in a magnesium oxide bi-crystal to the polarisation of an applied microwave field as a function of temperature.

Acknowledgments The authors acknowledge the support of the Engineering and Physical Sciences Research Council.

Corresponding Author: Neil McN Alford n.alford@imperial.ac.uk

I Introduction

One question that has never been convincingly answered is whether grain boundaries in polycrystalline ceramics influence dielectric loss. In microwave filters and a range of communications devices, low dielectric loss is essential for good performance, so this question is an important one to address. Single crystals often exhibit superior properties in comparison with their polycrystalline analogues. Single crystal whiskers of alumina can approach their theoretical tensile strength of 40 GPa, approximately 10% of the Young Modulus E^1 , while the strength of polycrystalline alumina is usually around 0.4 GPa. In polycrystalline ceramic materials, strength is usually dictated by processing defects that act as critical flaws², limiting tensile strength to around 0.1% of E . When these processing defects are absent, strength is governed by the length of the largest grain boundaries³. The relation between electrical properties and grain size in electroceramics is not clear since there are conflicting views regarding the effect of grain size on microwave dielectric loss. The general opinion though is that grain boundaries *do* have an adverse effect on microwave dielectric loss. It is not surprising then, that grain boundaries have been held responsible for contributing to the dielectric loss in ceramic materials.

The huge differences in microstructure and perfection between single crystals and their polycrystalline analogues are clear indicators why the conventional wisdom has assumed the impossibility of achieving a dielectric loss in polycrystalline ceramics approaching that of single crystals. Earlier studies have demonstrated the deleterious effects of impurities and it is certainly true that even minor amounts of impurity will cause huge increases in dielectric loss⁴. The problem though, is that because impurities have such a major influence, it is difficult to isolate the effect of grain boundaries. This is particularly the case in polycrystalline ceramics where the sintering process sweeps impurities to grain boundaries so that impurities and grain boundaries are inextricably linked. In the work described below we restrict our analysis to a material with a low relative permittivity on the grounds that ferroelectric materials possess additional loss mechanisms that complicate the discussion. The experiment described is carried out on MgO with a relative permittivity of less than 10.

1
2
3 Dielectric loss is described by the imaginary part of the permittivity, or more commonly by its
4 ratio to the real part, the loss tangent $\tan\delta$. The problem of dielectric loss at high frequency was
5 studied by Lord Rayleigh who published a paper in 1897 on dielectric waveguides⁵ and in 1909
6 by Debye on the subject of dielectric spheres⁶. Losses in bulk crystals fall into two categories,
7 intrinsic and extrinsic. Intrinsic losses are dependent on the crystal structure and can be
8 described by relaxation of the non-equilibrium phonon distribution created by an alternating
9 electric field^{7,8,9}. These intrinsic losses set the lower limit of losses found in pure 'defect free'
10 single crystals. Extrinsic losses are associated with imperfections in the crystal structure, e.g.
11 impurities, microstructural defects, grain boundaries, porosity, microcracks and random
12 crystallite orientation. It is clear from our experiments, and those of others, that the loss in
13 sintered ceramics is limited by these extrinsic losses but the precise influence of grain boundaries
14 has never been determined.
15
16
17
18
19
20
21
22
23
24

25
26
27 It seems reasonable to assume that if grain boundaries are a source of dielectric loss, then
28 reducing their number might be expected to reduce the dielectric loss. The logical extension of
29 this assumption is the case of single crystals that do indeed show very low loss^{7,10} but this
30 assumption is incorrect. Ceramic materials have been observed to show grain size dependence
31 but this relationship is not straightforward. Kim *et al*¹¹, in a study of Ni-doped $\text{Ba}(\text{Ni}_{1/3}\text{Nb}_{2/3})\text{O}_3$
32 found that the $\tan\delta$ decreased as the grain size increased. However, the system was complicated
33 by the fact that there were porosity variations, ordering parameter variations and the possible
34 presence of a liquid phase associated with an increase in $\tan\delta$. Ichinose *et al*¹² found that the $\tan\delta$
35 in $\text{Ba}(\text{Mg}_{1/3}\text{Ta}_{2/3})\text{O}_3$ ceramics decreased as grain size increased, saturating at a grain size of
36 around 9 μm . Kim *et al*¹³ found that ordering played a dominant role in the dielectric loss of
37 $\text{Ba}(\text{Mg}_{1/3}\text{Ta}_{2/3})\text{O}_3$ so that again, grain size effects were masked. However in the region where
38 ordering was constant (at the lower sintering temperatures), they found an increase in $\tan\delta$ as
39 grain size decreased. The problem with such perovskite systems is that the interplay of so many
40 properties such as grain size, porosity, cation ordering and liquid phases makes it difficult to
41 make definitive remarks on the relationship between grain size and loss. In a study of BiVO_5 ,
42 Prasad *et al*¹⁴ found that the dielectric constant and dielectric loss (at 100 kHz) increased with
43 increasing grain size but the problem in this study was that the density also varied significantly
44 making a firm correlation between grain size and dielectric properties unreliable. Chen *et al*¹⁵ in
45
46
47
48
49
50
51
52
53
54
55
56
57
58
59
60

1
2
3 a study of $\text{Ca}(\text{Zn}_{1/3}\text{Nb}_{2/3})\text{O}_3$ ceramics found that the dielectric loss decreased as the grain size
4 increased. This was attributed to a decrease in the length of grain boundaries and hence the
5 lattice defects in the vicinity of the grain boundary. However, they also suggested that there was
6 a greater oxygen deficiency in ceramics with larger grains. On annealing in oxygen an
7 improvement in Q factor of around 30% was observed. Unfortunately no evidence regarding the
8 degree of oxygen deficiency or lattice defects was given. In ZnO doped $\text{CaTi}_{1-x}(\text{Fe}_{1/2}\text{Nb}_{1/2})_x\text{O}_3$,
9 Kucheiko *et al*¹⁶ found that the $\tan\delta$ decreased with increasing grain size but in the undoped
10 material the grain size did not influence $\tan\delta$. In ferroelectric materials such as BaTiO_3 the effect
11 of grain size on ferroelectricity is rather complex but in general there is a decreased $\tan\delta$ with
12 decreasing grain size, however there is a significant frequency dependence associated with the
13 resonant frequency of the domains which masks the real relation between microwave loss and
14 grain size. In PbTiO_3 grain size plays an important role in governing domain switching, but
15 again the correlation with grain size is complex¹⁷. Alford *et al*⁴ studied polycrystalline Al_2O_3 ,
16 where the density remained constant at 98.1 ± 0.5 % of theoretical density and cation ordering,
17 liquid phases and ferroelectricity were absent. Within the accuracy of the measurement the
18 relative dielectric constant displayed no variation with grain size. The same was not true for the
19 $\tan\delta$. It was expected that as the grain size increased, the $\tan\delta$ would decrease because a
20 reduction in the number of grain boundaries per unit volume would result in a material with a
21 lower loss. In fact the $\tan\delta$ remained constant at approximately 2.5×10^{-5} for samples with a grain
22 size less than about $3 \mu\text{m}$ and then increased linearly as grain size increased to a value of 10^{-4} at 7
23 μm . In a theoretical treatment, Schlomann¹⁸ analysed the losses expected in ionic crystals with
24 disordered charge distributions and concluded that their contribution to loss (in magnetic spinels
25 at least) would be negligible unless the grain size was extremely small. He assumed a very small
26 average grain size of $0.01 \mu\text{m}$ suggesting that most ceramic materials would not be affected by
27 these losses. This is highly likely on the grounds that the average grain size in microwave
28 dielectric ceramics is usually much greater than $0.01 \mu\text{m}$.
29
30
31
32
33
34
35
36
37
38
39
40
41
42
43
44
45
46
47
48
49
50
51
52
53
54
55
56
57
58
59
60

II Experimental Procedure

(1) *Microscopy*

We examined the microstructure and electrical characteristics, (relative permittivity and the $\tan\delta$ as a function of temperature) of MgO single crystal and bi-crystal spheres of 10mm diameter. Single crystal spheres of MgO were cut from a large single bi-crystal (PDCrystals, Netherlands) grown by an arc-image furnace technique. The cut was arranged such that some of the spheres possessed a single grain boundary through their equator and some possessed no grain boundary. In order to examine the microstructure of the grain boundary we sliced the MgO sphere using a diamond saw and polished the face. The grain boundary was examined by polarised light optical microscopy and by transmission electron microscopy (FEI Titan 80/300).

(2) *Electrical Measurements*

For the electrical characterisation we used a dielectric resonator technique where a MgO sphere is placed inside a cylindrical silver-plated brass cavity on a low-loss single crystal quartz ring support structure. The MgO sphere was held in place by a thin PTFE piston rod which was secured by a steel spring as shown in Figure 1.

Coupling microwave energy into the sphere was achieved via two antenna loops protruding from the side of the cavity and oriented so as to excite or probe an axial magnetic field component. The conductivity of the silver plated cavity was characterised by measuring the unloaded quality factor Q_0 of the TE_{011} mode in the empty cylindrical cavity as a function of temperature. The conductivity of the cavity at room temperature was $5.94 \times 10^7 \Omega^{-1}m^{-1}$. The diameter D of the cylindrical cavity was 24.00 mm and its height H was 16.10 mm. The $TE_{01\delta}$ fundamental mode was used due to its high electric energy filling factor, low conductor losses and axisymmetric field distribution. Also, the effect of the PTFE rod could be neglected due to the very small electric filling factor along the cavity axis. The use of this mode allows the electric field to be parallel or normal to the grain boundary when the sphere is aligned vertically or horizontally with respect to the cavity axis. The quartz was cut (001) so that the axial component of its uniaxial

1
2
3 anisotropic permittivity was commensurate with the cavity. Transmission measurements of the
4 resonant frequency and quality factor were performed on an Agilent HP8720C Vector network
5 analyser with 1 Hz resolution. The measurements were performed over the temperature range
6 25-300K by placing the cavity on the cold head of a closed cycle Gifford McMahon cooler
7 (Cryophysics).
8
9
10
11

12 13 14 15 16 17 18 19 20 21 22 23 24 25 26 27 28 29 30 31 32 33 34 35 36 37 38 39 40 41 42 43 44 45 46 47 48 49 50 51 52 53 54 55 56 57 58 59 60

III Results and Discussion

(1) *Transmission Electron Microscopy*

The grain boundary is seen in fig 2, a high resolution TEM photo of the boundary. It is a remarkably clean interface and there is no evidence of a second phase or amorphous phase at the grain boundary.

(2) *Electrical Measurements*

A multi-region, multi-layer radial mode matching technique for axisymmetric cylindrical structures^{19, 20} was used to calculate the relative permittivity ϵ_r and loss tangent $\tan\delta$ using the measured data. A linear system of equations can be solved for the unknown permittivity given the resonant frequency. For axisymmetric cylindrical modes, the problem of modelling the resonator is reduced to a two dimensional one. Unfortunately, the stair-casing problem occurs when attempting to model the curved surfaces of a sphere using rectilinear regions. To overcome this, a method suggested by Hui²¹ was used where the average results were taken for two approximations, where the stepped outline of the rectilinear approximation is either circumscribed or inscribed by the cross-section of the sphere. A convergence study was then conducted to find the optimum number of modes required. The $\tan\delta$ of a quartz single crystal at room temperature²² is of the order of 2×10^{-5} . Krupka *et al*¹⁰ demonstrated that the temperature dependence of the losses in single crystal quartz are complex over the range 10–300 K but fairly constant over the 10-100 K range at around 1.2×10^{-5} . The permittivity normal to the axis, $\epsilon_t=4.43$, only varies by $\pm 0.06\%$ over the same temperature range. These data for single crystal quartz were used in the calculations. At room temperature, the resonant frequency of the quasi-TE₀₁₈ mode was measured at 9.3726 GHz and had an unloaded Q factor of 61,877. The relative

permittivity ϵ_r , of the MgO sphere was calculated using the radial mode matching technique to be 9.64.

The unloaded quality factor of the resonator is modelled by

$$Q^{-1} = p_d \tan \delta + p_s \tan \delta + \frac{R_s}{G} \quad (1)$$

where p_d , $\tan \delta_d$ and p_s , $\tan \delta_s$ are the electric filling factor and loss tangent of the dielectric sphere and the spacer respectively, R_s is the surface resistance of the silver plated cavity and G is its geometric factor. The electric filling factors can be calculated by considering the fraction of electric energy residing in the dielectric with respect to the total electric energy:

$$p_i = \frac{\iiint_{V_i} \epsilon_r |\mathbf{E}|^2 dV}{\iiint_V \epsilon_r(V) |\mathbf{E}|^2 dV} \quad (2)$$

For this case the filling factors for the MgO sphere and the quartz spacer were found to be $p_d = 0.8629$ and $p_s = 0.0476$, which shows that the MgO contains the bulk of the electric energy residing within the cavity. The geometric factor is evaluated from the expression:

$$G = \frac{\iiint_V \mu_0 |\mathbf{H}|^2 dV}{\iint_S |\mathbf{H}_t|^2 dS} \quad (3)$$

which involves volume and surface integrals of the magnetic fields. The geometric factor G for the cavity was calculated to be 2373. The room temperature surface resistivity R_s was measured to be 29.5 m Ω , yielding conductor losses of 1.243×10^{-5} which correspond to a conductor quality factor Q_c of 80,441. The loss tangent of the MgO sphere can then be calculated by rearranging (1):

$$\tan \delta_d = \frac{1}{p_d} \left(\frac{1}{Q_0} - p_s \tan \delta_s - \frac{R_s}{G} \right) \quad (4)$$

The permittivities of MgO where the grain boundary was aligned vertically or horizontally with respect to the cavity axis were measured as a function of temperature, and are almost identical as

1
2
3 shown in Figure 3a. There was no significant difference in the relative permittivity of any of the
4 spheres whether or not they contained a grain boundary.
5
6

7
8 The loss tangent, $\tan\delta$ for the spheres shown in Figure 3b. The orientation of the grain boundary,
9 whether it is vertical or horizontal with respect to the cavity axis makes no difference to the
10 measured loss. There is virtually no difference in the $\tan\delta$ between any of the samples above 75K
11 . At around 45K there is a pronounced peak in the $\tan\delta$ for the bi-crystal which is absent for the
12 single crystal. This peak is attributed to defect dipole relaxation of oxygen ions between oxygen
13 vacancies. This phenomenon has been reported by Zuccaro et al²³ in the case of oxygen
14 vacancies in LaAlO₃ caused by twin boundary defects.
15
16
17
18
19

20
21 The losses due to defect dipole Debye relaxation of oxygen ions at the grain boundary can be
22 modelled using the following expression:
23

$$\tan \delta = \frac{\Delta \varepsilon}{\varepsilon_r \varepsilon_0} \left(\frac{\omega \tau}{1 + \omega^2 \tau^2} \right) \quad (5)$$

24
25
26
27
28
29 Where $\Delta \varepsilon = \eta N_d p^2 / k_B T$, where η is the field correction factor, N_d is the defect density, and p is
30 the defect dipole moment. The thermally activated relaxation time τ is given by
31 $\tau = \tau_0 \exp(E / k_B T)$. A single Debye peak was fitted to the observed difference in loss tangent
32 between a single crystal and bi-crystal but was found not to describe the data accurately. Twin
33 Debye relaxation peaks were then fitted and a good agreement was found with experimental data
34 as shown in Figure 4.
35
36
37
38
39
40

41
42 The total defect density was found to be $1.24 \times 10^{12} \text{ cm}^{-3}$, with approximately equal contribution
43 from the two peaks. The defect dipole activation energies for the peaks were found to be 14.9
44 and 18.3 meV and the relaxation times 73.6 and 149.0 fs respectively. These results suggest that
45 dielectric losses at low temperatures are sensitive to very small concentrations of defects and that
46 this measurement technique is capable of detecting and quantifying them.
47
48
49
50

51
52 The temperature dependence of the $\tan\delta$ indicates that there is a small contribution at low
53 temperature which we interpret to be caused by Debye relaxation. The very low activation
54 energies (<20 meV) suggest that a collective motion of ions is responsible for the observed
55 losses.
56
57
58
59
60

IV Conclusions

The propensity for grain boundaries in polycrystalline ceramics to act as a sink for impurities, which do indeed have a deleterious effect on loss, is the main reason why grain boundaries have been held as the main contributors to dielectric loss. In the experiments carried out here on clean grain boundaries in MgO crystals, the influence on microwave loss is only seen at low temperatures. The temperature dependence of the $\tan\delta$ indicates that there is a small contribution at low temperature which we interpret to be caused by Debye relaxation.

The overall conclusion from this work is that grain boundaries have a very limited influence on the microwave dielectric loss. A single grain boundary in MgO has no effect on the microwave dielectric loss at room temperature and a very slight effect at low temperature (around 45K). Further, at room temperature, the difference in microwave loss between very pure single crystals and their polycrystalline counterparts is small and this has been shown to be the case in a number of ceramic dielectric materials including Al_2O_3 , TiO_2 , MgO and LaAlO_3 ^{4, 24,25,26}. In these studies it was found that impurities and porosity were particularly deleterious to microwave loss.

Figure Captions

Fig 1 Dielectric resonator consisting of spherical MgO bi-crystal (diameter =10 mm), inside a cylindrical silver-plated cavity ($D = 24.00$ mm, $L = 16.10$ mm), placed upon single crystal quartz support ring ($r = 5$ mm, $R = 10$ mm, $l = 4$ mm). The centre of the sphere is situated at a distance $h = 8.33$ mm from the bottom of the cavity.

Figure 2 High Resolution TEM image of the grain boundary interface.

1
2
3 Figure 3a Relative permittivity of MgO measured over 25-250K temperature range for vertical
4 (V) and horizontal (H) grain boundary alignments.
5
6

7
8 Figure 3b. Measured $\tan\delta$ for vertical and horizontal alignments of the single grain boundary in a
9 spherical MgO bi-crystal together with a grain boundary free MgO sphere. The small peak in
10 $\tan\delta$ for samples containing a grain boundary at around 45K which is thought to be due to defect
11 dipole relaxation of oxygen vacancies
12
13
14

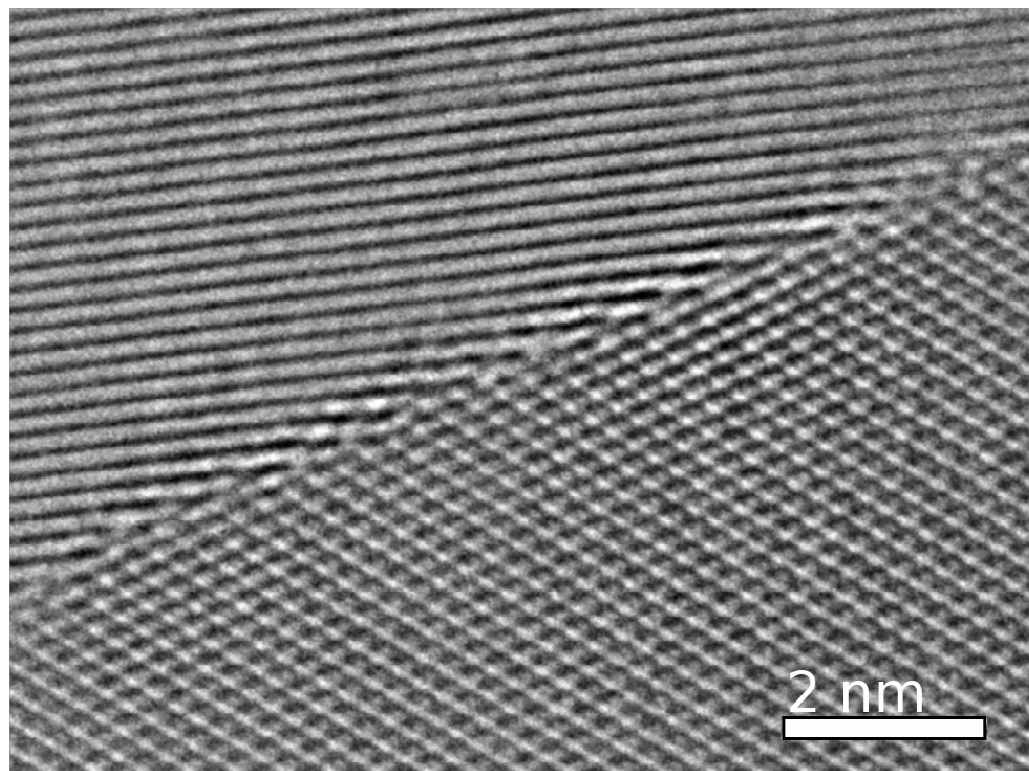
15
16 Figure 4. Difference in loss tangent $\Delta\tan\delta$ between a MgO bi-crystal containing a single grain
17 boundary and a grain boundary free MgO single crystal. Both samples were spherical and
18 resonated at 9.37 GHz. Multiple Debye peaks were fitted to the observed peak.
19
20
21
22
23
24
25

26 References

- 27
28
29 ¹ Cottrell, A.H. Strong Solids. *Proc. Royal Soc.* **A282**, 2–9 (1964).
30 ² Griffith, A.A. The phenomenon of rupture and flow in solids. *Phil. Trans. Roy. Soc.* **221**, 163–
31 198 (1920).
32 ³ Alford, N.M., Birchall, J.D. & Kendall, K. High-strength ceramics through colloidal control to
33 remove defects. *Nature* **330**, 51–55 (1987).
34 ⁴ Alford, N.M. & Penn, S.J. Sintered alumina with low dielectric loss. *Journal of Applied Physics*
35 **80**, 5895–5898 (1996).
36 ⁵ Lord Rayleigh. *Phil. Mag. S. 5* **43**, 125–132 (1897).
37 ⁶ Debye, P. Lichtdruck auf Kugeln von bliebigem Material. *Annalen der Physik* **30**, 57–136
38 (1909).
39 ⁷ Braginsky, V.B. & Ilchenko, V.S. Experimental observation of fundamental microwave
40 absorption in high-quality dielectric crystals. *Physics Letters A* **120**, 300–305 (1987).
41 ⁸ Gurevich, V.L. & Tagantsev, A.K. Intrinsic dielectric loss in crystals. *Advances in Physics* **40**,
42 719–767 (1991).
43 ⁹ Sparks, M., King, D.F., & Mills, D.L. *Phys. Rev. B* **26**, 6987 (1981).
44 ¹⁰ Krupka, J., Derzakowski, K., Tobar, M., Hartnett, J. & Geyer, R. G. Complex permittivity of
45 some ultralow loss dielectric crystals at cryogenic temperatures. *Measurement Science &*
46 *Technology* **10**, 387–392 (1999).
47 ¹¹ Kim, I.-T., Kim, Y. & Chung, S.J. Order-disorder transition and microwave dielectric
48 properties of Ba(NiNb)O ceramics. *Japanese Journal of Applied Physics* **34**, 4096–4103 (1995).
49 ¹² Ichinose N. and Shimada T., Effect of grain size and secondary phase on microwave dielectric
50 properties of Ba(Mg_{1/3}Ta_{2/3})O₃ and Ba([Mg,Zn]_{1/3}Ta_{2/3})O₃ systems. *J. Europ. Ceram. Soc.* **26**,
51 1755–1759 (2006).
52 ¹³ Kim, E.S. & Yoon, K.H. Effect of nickel on microwave dielectric properties of Ba(MgTa)O.
53 *Journal of Materials Science* **29**, 830–834 (1994).
54
55
56
57
58
59
60

- 1
2
3
4
5
6
7
8
9
10
11
12
13
14
15
16
17
18
19
20
21
22
23
24
25
26
27
28
29
30
31
32
33
34
35
36
37
38
39
40
41
42
43
44
45
46
47
48
49
50
51
52
53
54
55
56
57
58
59
60
- ¹⁴ Prasad, K. V.R., Raju, A.R. & Varma, K. B.R. Grain size effects on the dielectric properties of ferroelectric BiVO ceramics. *Journal of Materials Science* **29**, 2691–2696 (1994).
- ¹⁵ Chen, X.M., Liu, D., Hou, R.Z. & Hu, X. Microstructures and Microwave Dielectric Characteristics of Ca(ZnNb)O ceramics. *Journal of the American Ceramic Society* **87**, 2208–2212 (2004).
- ¹⁶ Kucheiko, S., Kim, H.-J., Yoon, S.-J. & Jung, H.-J. Effect of ZnO additive on the microstructure and microwave dielectric properties of CaTi(FeNb)O ceramics. *Japanese Journal of Applied Physics* **36**, 198–202 (1997).
- ¹⁷ McNeal, M.P., Jang, S.-J. & Newnham, R.E. The effect of grain and particle size on the microwave properties of barium titanate BaTiO. *Journal of Applied Physics* **83**, 15 (1998).
- ¹⁸ Schlomann, E. “Dielectric Losses in ionic crystals with disordered charge distributions” *Phys Rev B* **35** (2a) p A413 – A419 (1964)
- ¹⁹ Wang, C. & Zaki, K.A. Generalized multilayer anisotropic dielectric resonators. *IEEE Trans. Micro. Theory Tech.* **48**, 60 (2000).
- ²⁰ Kajfez, D. & Guillon, P. *Dielectric Resonators* (Artech House, 1986).
- ²¹ Hui, W.K. & Wolff, I. A Multicomposite, Multilayered Cylindrical Dielectric Resonator for Application in MMIC’s. *IEE-MTT* **42**, 361 (1994).
- ²² Zychowicza, T., Krupka, J. & Tobar, M.E. Whispering gallery modes in hollow spherical dielectric resonators. *J. Eur. Ceram. Soc.* **26**, 2193–2194 (2006).
- ²³ Claudio Zuccaro, Michael Winter, Norbert Klein, and Knut Urban “Microwave absorption in single crystals of lanthanum aluminate” *Journal of Applied Physics* -- December 1, 1997 -- Volume 82, Issue 11, pp. 5695-5704
- ²⁴ Jonathan D. Breeze, Xavi Aupi and Neil McN. Alford. “Ultra-Low Loss Polycrystalline Alumina” *Appl Phys Lett* vol 81 p 5021 (2002)
- ²⁵ Templeton Alan Templeton, Xiaoru Wang, Stuart J Penn, Stephen J Webb, Lesley F Cohen and Neil McN Alford “Microwave Dielectric Loss of Titanium Oxide” *J Amer Ceram Soc* **83** (1) 95-100 (2000).
- ²⁶ N.McN. Alford, J Breeze, X Wang, SJ Penn, S Dalla, SJ Webb, N Ljepojevic and X Aupi. “Dielectric Loss of oxide single crystals and polycrystalline analogues from 10 to 320K” *J European Ceramic Society* vol 21 pp 2605-2611 (2001)

Fig 1



1
2
3
4
5
6
7
8
9
10
11
12
13
14
15
16
17
18
19
20
21
22
23
24
25
26
27
28
29
30
31
32
33
34
35
36
37
38
39
40
41
42
43
44
45
46
47
48
49
50
51
52
53
54
55
56
57
58
59
60

Fig 2

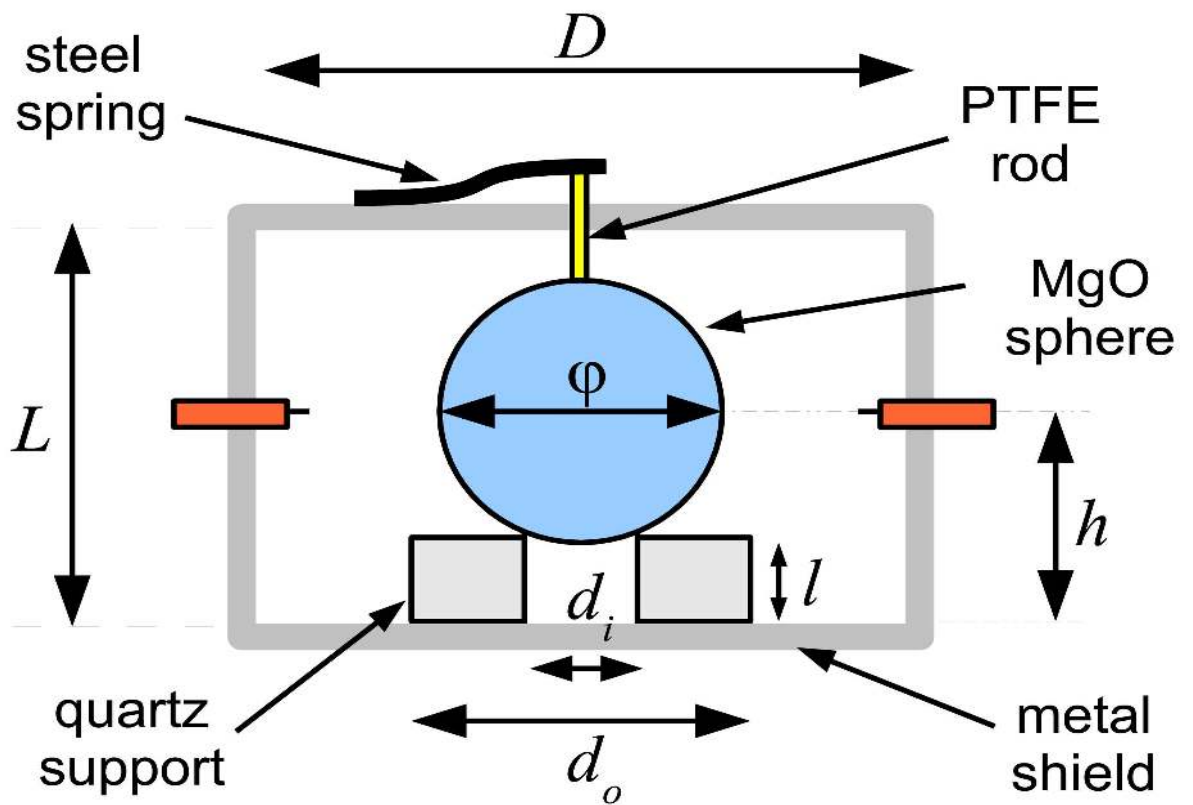
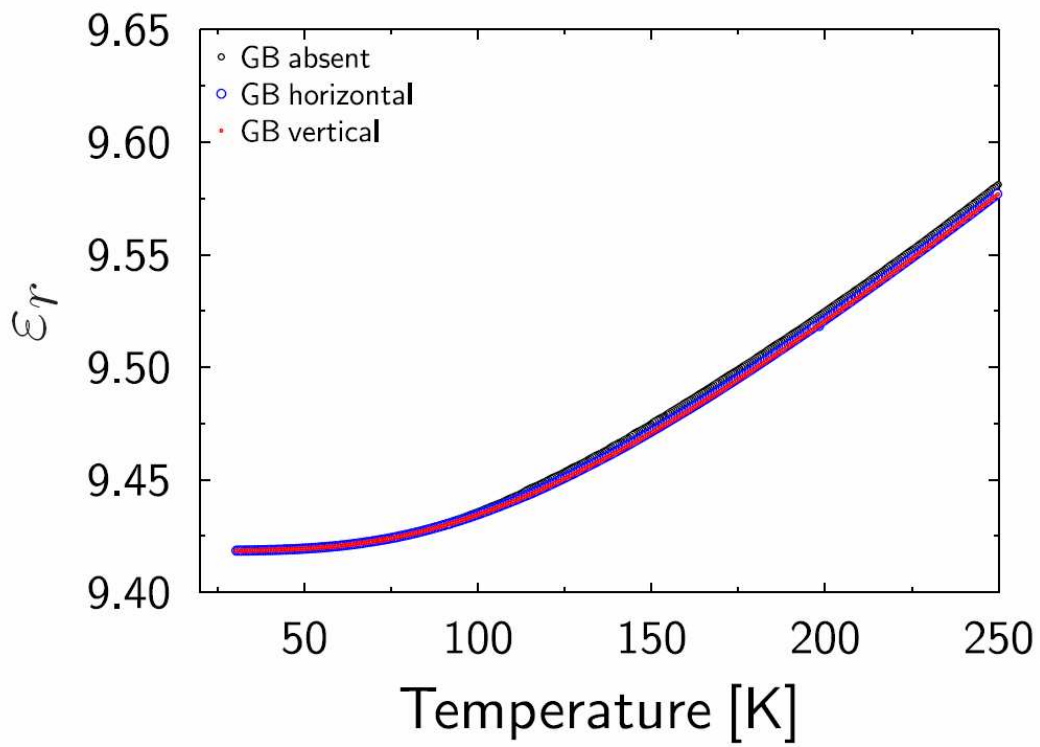
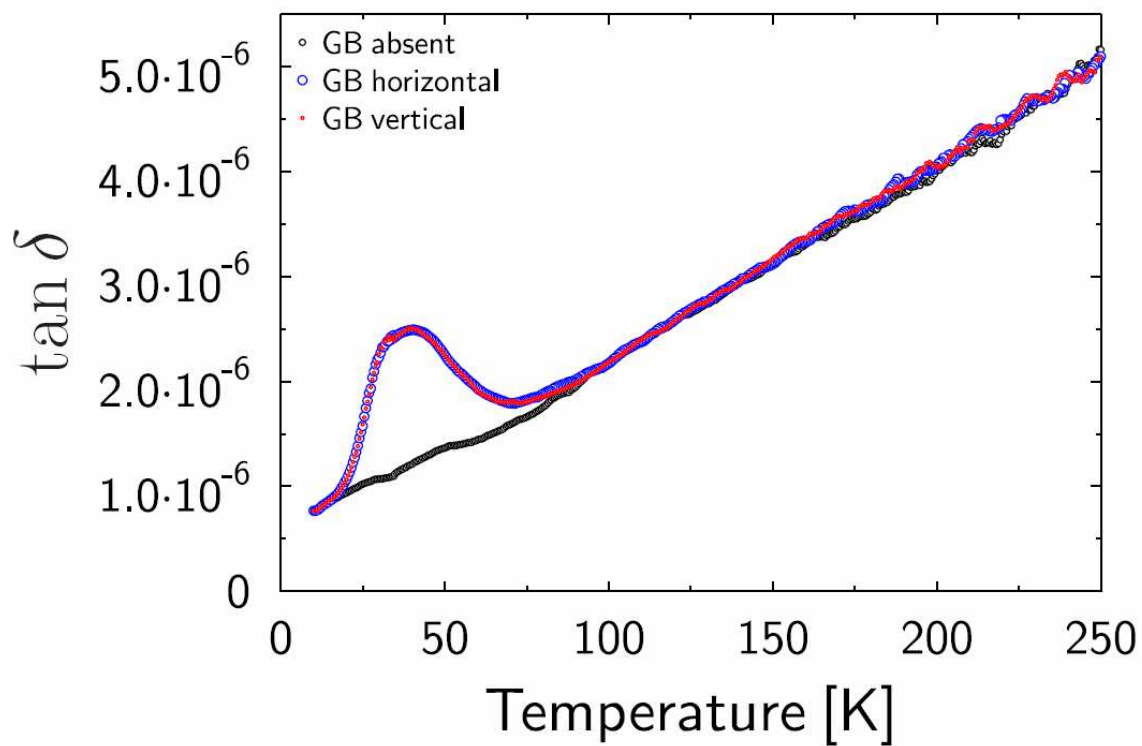


fig 3a



Peer Review

fig 3b



er Review

fig 4

